Results in Surfaces and Interfaces 19 (2025) 100551

Contents lists available at ScienceDirect

Results in Surfaces and Interfaces

journal homepage: www.elsevier.com/locate/rsurfi

Diffusion-driven $L1_0$ FePt phase formation in Fe/Ag(Au)/Pt and Pt/Ag(Au)/Fe trilayers with inverted layer stacking

G.L. Katona [a], P.V. Makushko [b,d], N.Y. Schmidt [c], O. Lik [c], T.I. Verbytska [b], G. Beddies [c], D.L. Beke [a], M. Albrecht [c], Yu.M. Makogon [b,*]

[a] Department of Solid State Physics, Faculty of Sciences and Technology, University of Debrecen, P.O. Box 400, H-4002, Debrecen, Hungary
[b] Department of Physical Materials Science and Heat Treatment, National Technical University of Ukraine "Igor Sikorsky Kyiv Polytechnic Institute", Prospect Beresteiskyi 37, Kiev, 03056, Ukraine
[c] Institute of Physics, University of Augsburg, Universitätsstrasse 1, 86159 Augsburg, Germany
[d] Helmholtz-Zentrum Dresden-Rossendorf e.V., Institute of Ion Beam Physics and Materials Research, 01328, Dresden, Germany

ARTICLE INFO

Keywords:
Vacuum annealing
Diffusion paths
Layer stacking sequence
Ordering
$L1_0$ FePt
Coercivity
Magnetization

ABSTRACT

In this work the diffusion-induced formation of an ordered $L1_0$ FePt phase in Fe(15 nm)/Ag(Au)(10 nm)/Pt(15 nm) and Pt(15 nm)/Ag(Au)/Fe(15 nm) trilayers with a Ag(Au) interlayer upon annealing is studied. The films were prepared by magnetron sputtering on SiO_2/Si(001) substrates. Isothermal annealing of the samples was carried out in vacuum at 700°C for different annealing times up to 30 min. It was found that the stacking sequence of the trilayer has a strong impact on the direction of the diffusion process. This results in the formation of different chemical composition along the film thickness which is explained by the different formation enthalpies of possible phases. Finally, the hard magnetic $L1_0$ FePt phase is formed with grain boundaries filled by Ag(Au) resulting in enhanced coercivity. In addition, depending on the layer stacking sequence, the remaining Ag(Au) can be found either on the top surface or at the substrate interface. In this regard, employing different diffusion paths on selected layer stacks is a promising approach of forming gradient nanomaterials with properties that might be useful for practical applications.

1. Introduction

Potential magnetic material candidates for spintronics and storage applications are chemically ordered $L1_0$ thin films such as FePt, FePd, and CoPt ([1–3]; Lubina et al., 2011; [4,5]; D. [6]). They are ferromagnetic and can exhibit strong magneto-crystalline anisotropy.

Their magnetic properties can be further tailored by adding third elements causing texture growth as well as magnetic grain isolation [7–16]. In this regard, the addition of Ag and Au elements has been found to strongly affect the structure and magnetic properties of FePt [2, 17–24,25–30].

During the formation process of the ordered $L1_0$ FePt phase, both Ag and Au are not incorporated in the crystal lattices of the $L1_0$ structure but are localized at the grain boundaries magnetically isolating the grains and thus resulting in a drastic increase of the coercive field. Additionally, a decrease in the onset temperature of the chemical ordering process of the $L1_0$ phase was observed.

In a recent study, we have investigated Fe/Ag/Pt thin films deposited on SiO_2(100 nm)/Si(100) substrates after long-term (up to 52 h) isothermal low-temperature treatment between 245 °C and 390 °C, as well as high-temperature annealing at 600 °C–900 °C for 30 s [28]. Composition profiles, obtained after isotherm heat treatment, showed that initially there is strong intermixing between Ag and Pt, resulting most likely in the formation of an Ag_xPt_{1-x} reaction layer. Furthermore, it was observed that the intermixing process was much faster in the Ag layer accompanied by the segregation of Ag to the substrate/Pt interface. Later on, the Pt, which diffused through the Ag layer, started to penetrate into the Fe grain boundaries. This process led to the formation of the FePt reaction product leaving behind an Ag layer next to the substrate. Furthermore, Pt/Au/Fe/sub. thin films deposited on Al_2O_3(0001) single crystalline substrates were investigated after long-term (up to 62 h) isothermal annealing in vacuum at 330 °C [31]. The introduction of an additional Au layer led to an enhanced diffusion process caused by grain boundary diffusion and the formation of the partially chemically ordered $L1_0$ FePt phase [27]. It was suggested that this enhancement of the diffusion process in presence of the Au

* Corresponding author.
E-mail address: Yurii_Makogon@ukr.net (Yu.M. Makogon).

https://doi.org/10.1016/j.rsurfi.2025.100551
Received 5 October 2024; Received in revised form 17 April 2025; Accepted 7 May 2025
Available online 10 May 2025
2666-8459/© 2025 The Authors. Published by Elsevier B.V. This is an open access article under the CC BY-NC-ND license (http://creativecommons.org/licenses/by-nc-nd/4.0/).

interlayer is promoted by stress accumulation. After the FePt alloy formation, Au was partially located in the grain boundaries of FePt and at the substrate interface. These different diffusion paths can be employed to form a concentration gradient associated with varying magnetic properties, as demonstrated in post-annealed asymmetric Pt/Fe/Pt/Au/Fe films [32]. In this case exchange coupled soft and hard magnetic phases along the film thickness were created.

Recently, attention has been paid to the influence of the layer stacking sequence. The stacking order strongly affects the formation of ordered $L1_0$ phase. So, for example, the addition of intermediate Ag layer promotes the formation of the FePd phase with $L1_0$ structure or $A1$ disordered structure depending on stacking order. By analysis of the chemical depth profiles and XRD patterns, the transformations were interpreted by diffusion induced grain boundary migration and solid state reaction [33].

Furthermore, in [34] the formation of the ordered $L1_2$ $FePd_3$ phase in Fe/Pd based thin films with Au intermediate layer was interpreted by the stress accumulation due to the different diffusivity of the components, which relaxes by the shift of the grain boundaries and the transformation of swept over regions. Interestingly, for samples with Mo buffer but without the Au interlayer the $L1_0$ FePd phase appeared depending on the stacking order.

The effect of layer stack inversion in Pt/Co based layer stacks on the diffusion processes was studied by [35]. Please note that no $L1_0$ CoPt phase formation is observed in these cases. However, also in this case the layer stacking has a pronounced effect on the diffusion rate especially at temperatures, where the diffusion is dominated by grain boundaries. An additional Au intermediate layer leads to an increase of the coercive field of the annealed samples due to a modification of exchange coupling between the magnetic grains at the grain boundaries [35].

Here, in the present study, the influence of the Fe and Pt position (top or bottom) in Fe/Ag(Au)/Pt and Pt/Ag(Au)/Fe trilayers with an Ag(Au) interlayer on the phase formation process upon post-annealing at 700 °C for 0.5 − 30 min was investigated.

2. Experimental

Trilayer thin films with reversed stacking sequences, Fe(15 nm)/Ag(Au)(10 nm)/Pt(15 nm)/sub. and Pt(15 nm)/Ag(Au)(10 nm)/Fe(15 nm)/sub., were prepared at room temperature by magnetron sputter deposition (Bestec GmbH) from individual Fe, Pt, Ag, and Au targets on SiO_2(100 nm)/Si(001) substrates. This ultra-high vacuum deposition system has a base pressure of $3{\cdot}10^{-5}$ Pa. Ar was used as sputter gas under a working pressure of $3.5{\cdot}10^{-1}$ Pa. The following sputter powers and deposition rates were applied: 107 W/0.04 nm/s for Fe, 43 W/0.05 nm/s for Pt, 12 W/0.05 nm/s for Ag, and 15 W/0.05 nm/s for Au.

The isothermal annealing of the samples at 700 °C was carried out in a vacuum chamber with a pressure $\sim 10^{-3}$ Pa. The annealing time was varied from 0.5 min, 2 min, 5 min, 15 min, and 30 min with heating and cooling rates of about 5 °C/s and 0.25 °C/s, respectively. The structural properties of the deposited and annealed films were characterized by X-ray diffraction (XRD) using an ULTIMA IV Rigaku diffractometer in standard (θ–2θ) geometry with Cu K_α radiation.

The degree of ordering of the $L1_0$ FePt phase was estimated from the intensity ratio of the $I(001)/I(002)$ of the fundamental (002) and superstructure (001) reflections. Depth profiles of the films were investigated by secondary neutral mass spectrometry (SNMS). In this experiment radio frequency Ar plasma at low pressure was used both as a source of bombardment ions and as a post-ionization medium. The low bombardment energy (350 eV) and the homogeneous plasma profile make it possible to obtain a depth resolution better than 2 nm. The concentration of elements was calculated under the assumption of a linear dependence of the measured intensity on the composition. Details of the SNMS setup and evaluation procedure can be found in Refs. ([36]; Peter et al., 2007). The magnetic properties were investigated by using a Superconducting Quantum Interference Device - Vibrating Sample Magnetometer (SQUID-VSM, Quantum Design GmbH).

3. Results and discussion

3.1. Phase formation and structural changes in Fe/Ag/Pt and Pt/Ag/Fe trilayers upon annealing

XRD (θ-2θ)-scans of Fe/Ag/Pt and Pt/Ag/Fe films after deposition and after annealing at 700 °C for different annealing times are shown in Fig. 1 (a) and 1 (b), respectively. In the diffractogram of the as-deposited Fe/Ag/Pt trilayer (Fig. 1 (a)), Pt(111), Ag(111), and Fe(110) peaks besides reflections from the substrate can be clearly observed. In contrast, in the as-deposited Pt/Ag/Fe trilayer additional orientations are revealed. Besides Pt(111), Ag(111), and Fe(110), pronounced Pt(200) and Ag(200) reflections are found, which might have an impact on the diffusion processes due to a different stress levels at the interfaces.

Fig. 2 shows the composition versus sputtering time profiles of the as-deposited Fe/Ag/Pt and Pt/Ag/Fe films and after annealing. As expected, the as-deposited trilayers can be well resolved without indication of interdiffusion (Fig. 2 (a)). The width of the interface regions corresponds to the depth resolution of the method.

After annealing at 700 °C for 0.5 min structural changes are clearly observed in both trilayer systems by XRD (Fig. 1 (a) and 1 (b)) revealing a decrease in the intensities of the individual layer reflections due to the mutual diffusion between the layers. This is confirmed by looking at the depth profiles presented in Fig. 2 (b). Strong diffusion in particular between the Ag and Pt layers is detected. This diffusion process is very pronounced in Fe/Ag/Pt, while in the Pt/Ag/Fe trilayer the average composition of Ag in the Pt layer and of Pt in the Ag layer is lower by about 6–8 at.% and 10–12 at.%, respectively. Here, Pt diffuses through the Ag layer, segregates at the Ag/Fe interface, and begins to dissolve into the Fe layer.

The process of mutual diffusion of Pt and Ag continues with increasing annealing time of 2 min (Fig. 2 (c)) where Pt strongly intermixes with Fe, while Ag in the Fe/Ag/Pt trilayer becomes unevenly distributed in the Fe–Pt solid solution and moves towards the substrate. In contrast, in the Pt/Ag/Fe trilayer, Ag is more homogenously distributed in the Fe–Pt solid solution with strong agglomeration at the top film surface. Further annealing of both trilayers only results in a more extended and more homogenous intermixing of Fe and Pt.

From the XRD patterns after 2 min of annealing (Fig. 1 (a) and 1 (b)) as a result of mutual diffusion between the layers there are significant changes in the phase composition in both films. All single layer reflections of Pt and Fe have disappeared while the characteristic reflection of the disordered $A1$ FePt(111) phase is observed confirming the formation of a solid solution. By increasing the annealing time further to 5 min, the additional appearance of a superstructural (001) reflection and a splitting of the fundamental cubic $A1$ (200) reflection into (200) and (002) (tetragonality) indicate the formation of an ordered $L1_0$ FePt phase in both films.

Furthermore, the presence of the Ag(111) and (200) reflection (the latter is only seen for the Pt/Ag/Fe trilayer) indicates that some amount of Ag remains as a separated layer. As expected, during the development of the diffusion-driven phase formation processes the Ag is not incorporated into the crystal lattice of both the disordered $A1$ FePt and ordered $L1_0$ FePt phase but remains partially in the grain boundaries of the FePt alloys. The ordered $L1_0$ FePt phase exists in the concentration range of 35–55 at. % according to the phase equilibrium diagram [37]. According to SNMS data, an ordered $L1_0$ FePt phase is formed with a composition near equiatomic (Fig. 2(c–f)). In combination with the depth profiles, it can be concluded that the Ag layer located near the substrate retains its (111) texture in the annealed Fe/Ag/Pt trilayer, while Ag located near the surface in the annealed Pt/Ag/Fe trilayer retains the predominant (200) texture.

Thus, a directed diffusion of the intermediate Ag layer towards the Pt layer is obtained in both films. This is also facilitated by the mutual

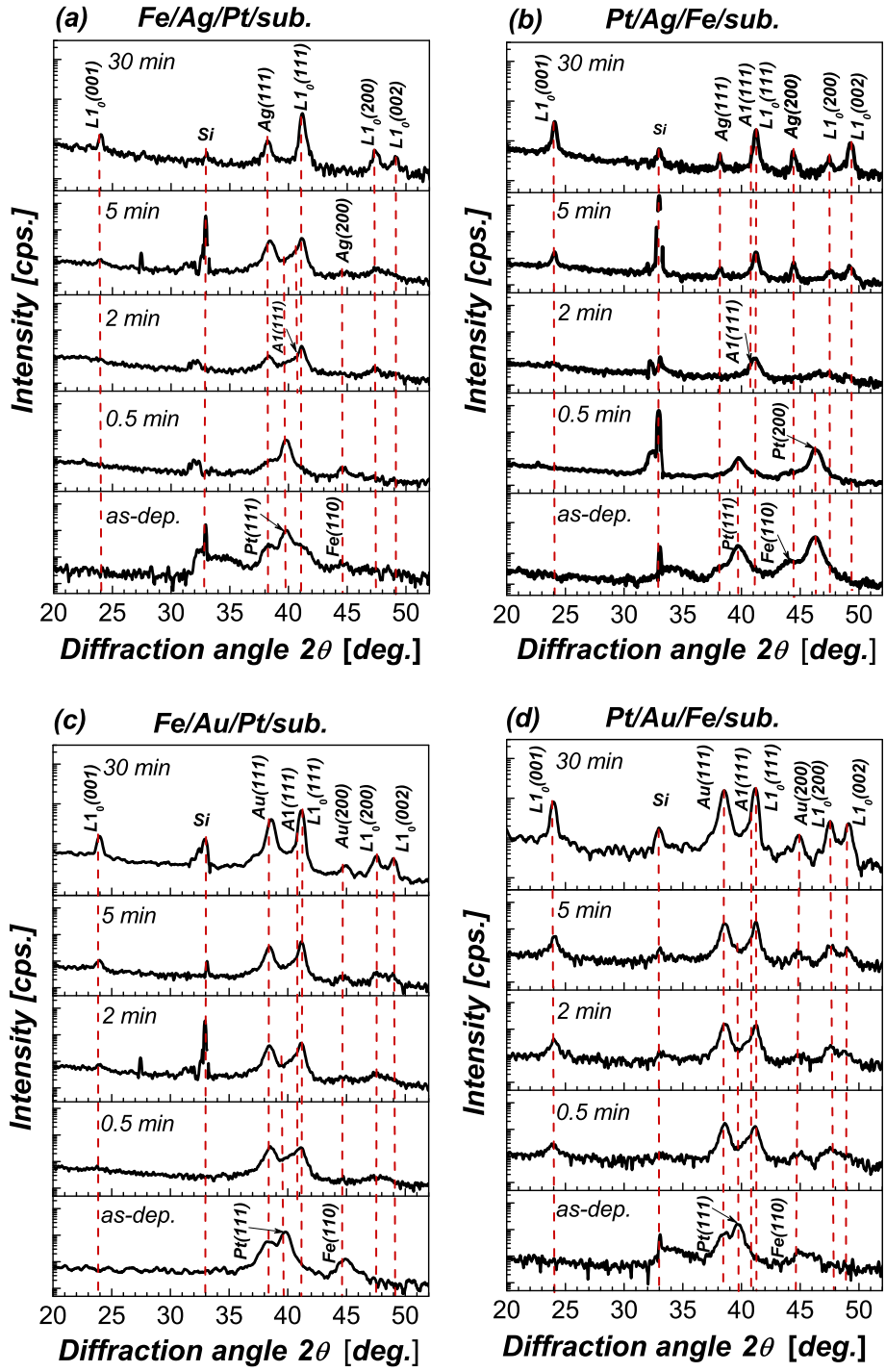

Fig. 1. X-ray diffraction patterns of as-deposited and post-annealed (700 °C for 0.5– 30 min) trilayers: (a) Fe(15 nm)/Ag(10 nm)/Pt(15 nm), (b) Pt(15 nm)/Ag(10 nm)/Fe(15 nm), (c) Fe(15 nm)/Au(10 nm)/Pt(15 nm), and (d) Pt(15 nm)/Au(10 nm)/Fe(15 nm).

insolubility of Ag and Fe. The degree of ordering of the $L1_0$ phase can be followed by the $I(001)/I(002)$ intensity ratio which basically increases with annealing time (Fig. 3 (a)). Please note that the diffusion and alloy formation process observed in Fe/Ag/Pt are quite similar to reported results on a similar layer stack annealed at temperatures between 600 °C and 900 °C for a short time of 0.5 min [28].

The room temperature *M-H* hysteresis loops of all samples in the as-deposited state (not shown) reveal a soft magnetic behavior of the Fe layers with an in-plane easy magnetization given by the magnetic shape anisotropy, similar to results reported in Ref. [28]. *M-H* hysteresis loops of the Fe/Ag/Pt and Pt/Ag/Fe films, which were annealed at 700 °C for 2 min and 30 min are presented in Fig. 4.

The films had insignificant magnetic anisotropy. The loops were presented in an out-of-plane applied magnetic field. As summarized in Fig. 3 (b), a strong increase in coercivity with annealing time is observed in both film systems which can be associated to the formation of the hard magnetic $L1_0$ FePt phase and in addition to the grain isolation induced by the filling of the grain boundaries with pure Ag.

From the presented results, it can be concluded that a different stacking order of Fe–Ag–Pt allows to form a film structure with a different underlaying microstructure as Ag always moves towards the Pt layer upon annealing. Since Ag does not dissolve in the formed $L1_0$-FePt

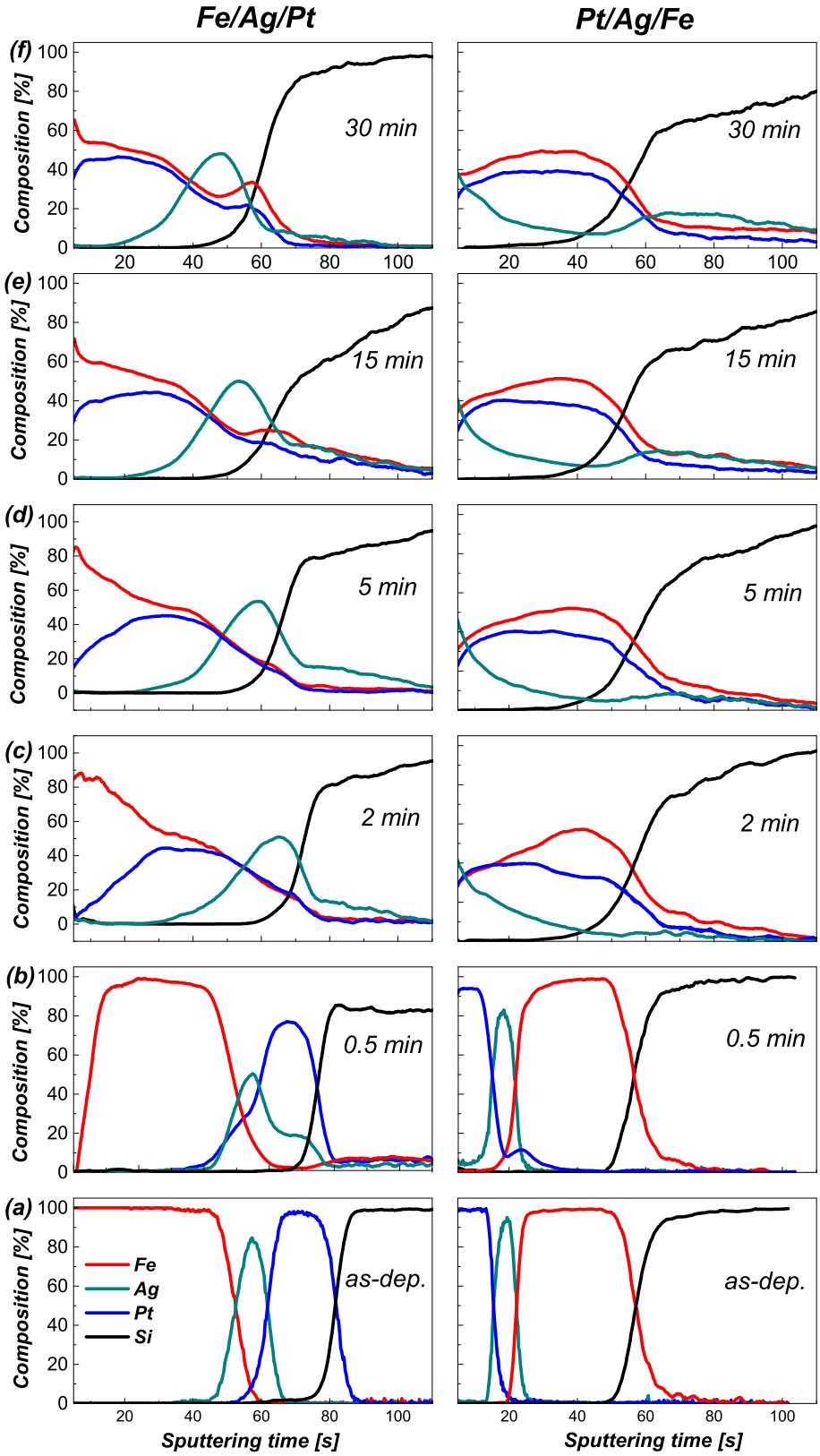

Fig. 2. Compositions versus sputtering time profiles of the (a) as-deposited Fe(15 nm)/Ag(10 nm)/Pt(15 nm) and Pt(15 nm)/Ag(10 nm)/Fe(15 nm) trilayers and (b–f) after annealing at 700 °C for different annealing times up to 30 min.

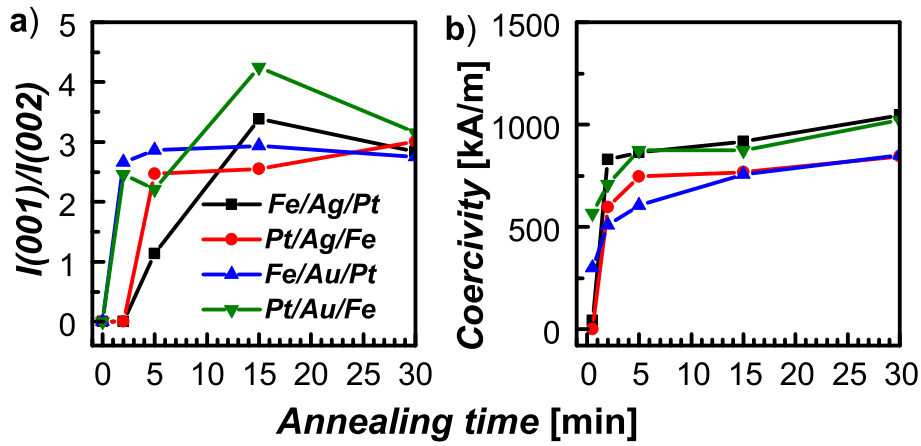

Fig. 3. Dependence of (a) *I(001)/I(002)* intensity ratio and (b) coercivity of Fe(15 nm)/Ag(Au)/Pt(15 nm) and Pt(15 nm)/Ag(Au)/Fe(15 nm) trilayers after post-annealing at 700 °C on the annealing time.

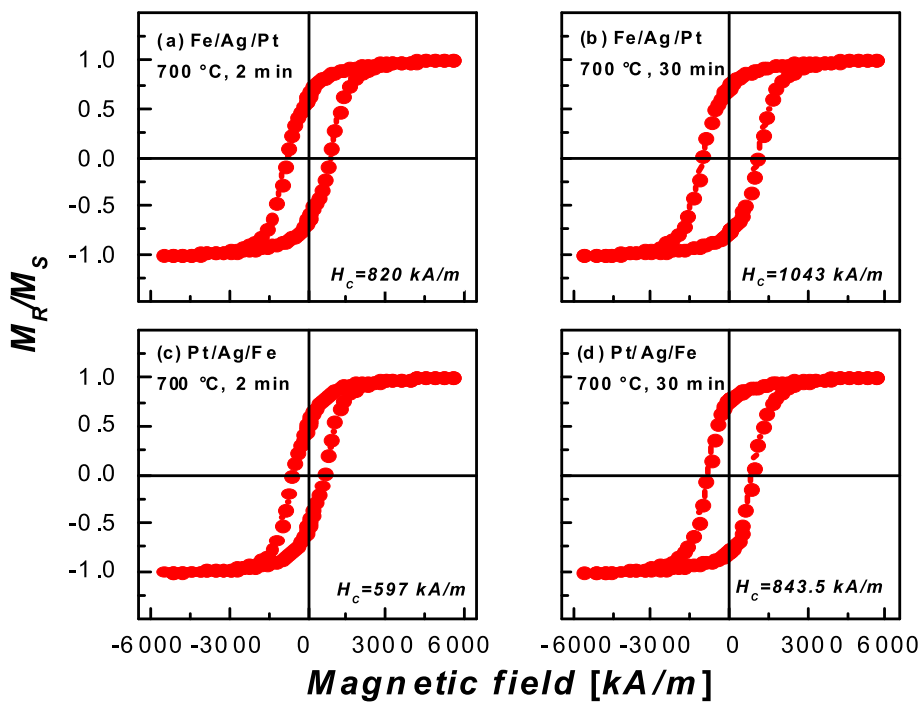

Fig. 4. Out-of-plane hysteresis loops of (a, b) Fe(15 nm)/Ag(10 nm)/Pt(15 nm) and (c, d) Pt(15 nm)/Ag(10 nm)/Fe(15 nm) films after post-annealing at 700 °C for 2 min and 30 min, respectively.

phase, Ag is located mainly at the grain boundaries and depending on the stacking order Ag is in addition displaced to the substrate interface for Fe/Ag/Pt or to the film surface for Pt/Ag/Fe resulting in a rather inhomogeneous Ag distribution in the annealed films.

3.2. Phase formation and structural changes in Fe/Au/Pt and Pt/Au/Fe trilayers upon annealing

The same investigation was performed for Fe/Pt-based trilayers using Au as intermediate layer. XRD patterns of Fe/Au/Pt and Pt/Au/Fe films after deposition and annealing at 700 °C for different annealing times up to 30 min are shown in Fig. 1 (c) and 1 (d), respectively. Only intensive peaks of Pt(111) and Au(111), and a weak peak of Fe(110) are presented in both films after deposition. Annealing for 0.5 min already leads to the onset of the formation of the hard magnetic $L1_0$ FePt phase, which is confirmed by the appearance of a low-intensity superstructural (001) reflection and fundamental (111) and (200) reflections in the XRD patterns. In this case, a significant part of the Pt has intermixed with Fe, which was not observed in case of interlayers with Ag. Thus, $L1_0$-FePt phase formation is strongly promoted by Au (see Fig. 3 (a)). Increasing the annealing time to 30 min leads to an increase in the intensity of the superstructural reflection and a clear splitting of the *A*l (200) reflection into $L1_0$ (200) and $L1_0$ (002). It can be noted that the position and intensity of the Au(111) reflection practically does not change, which confirms its insolubility in the lattices of the *A*l and $L1_0$ FePt phases. Qualitatively, the evolution of the XRD patterns of the two trilayers upon annealing appears rather similar.

However, compositions versus sputtering time profiles of Fe/Au/Pt and Pt/Au/Fe trilayers after deposition and annealing at 700 °C for different annealing times reveal a totally different behavior, as shown in Fig. 5. First, the layers of the as-deposited Fe/Au/Pt trilayer are well resolved. Though, the elemental profiles are all asymmetric including Si, which is believed to be due to a rough surface area of the substrate and not due to chemical intermixing of the layers (Fig. 5 (a)). After the first

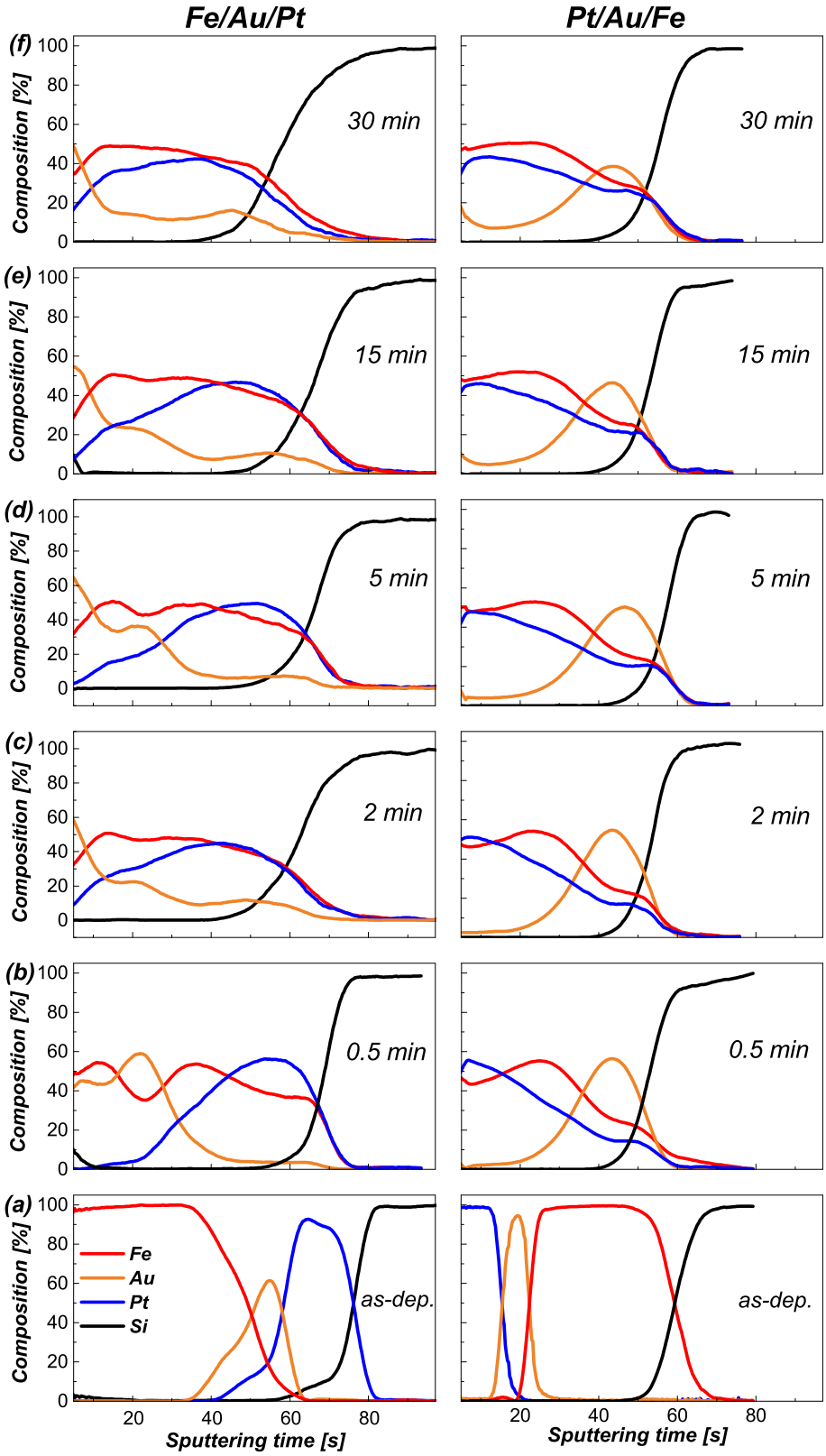

Fig. 5. Compositions versus sputtering time profiles of the (a) as-deposited Fe(15 nm)/Au(10 nm)/Pt(15 nm) and Pt(15 nm)/Au(10 nm)/Fe(15 nm) trilayers and (b–f) after annealing at 700 °C for different annealing times up to 30 min.

0.5 min (Fig. 5 (b)) of annealing, intensive interdiffusion between Fe and Au occurs.

Simultaneously, also Fe strongly intermixes with the Pt layer. Thus, Au–Fe and Fe–Pt solid solutions are mainly formed. Annealing for 2 min (Fig. 5 (c)) drastically changes the observed structure. Now Au segregates toward the surface and becomes more evenly distributed in the equiatomic FePt layer. Further annealing (Fig. 5(d–f)) leads to a further FePt layer homogenization. In this case, Au is mainly located along the

grain boundaries and at the top surface.

The layers of the as-deposited Pt/Au/Fe film are also well resolved and there is no apparent mutual diffusion between the layers (Fig. 5 (a)). After annealing for 0.5 min two Fe–Pt solid solutions are formed in the upper layers without Au and with Au near the substrate.

Thus, a rather uneven distribution of Au across the equiatomic FePt film is obtained. Annealing for 2–15 min only slightly changes the observed structure, which is consistent with the XRD results (Fig. 1 (d) and 5 (c-e)). With further increase in annealing time up to 30 min, Au segregation on the surface occurs during homogenization (Fig. 5 (f)).

Fig. 6 shows the *M-H* hysteresis loops applying an out-of-plane applied magnetic field of both trilayers after annealing. An increase in the *I(001)/I(002)* ratio of the $L1_0$ phase with the rise in the annealing time leads to an increase in the coercivity to 852 kA/m and 1019 kA/m in the Fe/Au/Pt and Pt/Au/Fe annealed trilayers, respectively (Figs. 3 and 6). The higher value of the coercivity in the Pt/Au/Fe film can be explained by the higher degree of chemical ordering.

Interestingly, by comparison of the two trilayer systems employing Ag and Au interlayers and looking again at the evolution of the depth profiles upon annealing (see Figs. 2 and 5), we can clearly see a similar behavior for Fe/Ag/Pt and Pt/Au/Fe as well as for Pt/Ag/Fe and Fe/Au/Pt. Thus, the situation is inverted with respect to Fe and Pt in the layer sequence. The reason is given by strong Fe–Au and Pt–Ag initial intermixing, as already observed in similar layer stacks [31,29,32].

This behavior can be partially explained by the higher negative enthalpy of mixing $\Delta H^{mix}_{(AB)}$ of the relevant atomic pairs (see Table 1), as calculated by Miedema's model [38].

Despite the more positive value of enthalpy of mixing for the Au–Fe diffusion pair (8 kJ/mol) compared to Au–Pt (4 kJ/mol), the diffusion of Fe into the Au layer is faster than that of Pt into Au, which can be explained by the significantly greater Fe solubility in Au than Pt in Au.

In contrast, for Fe/Ag/Pt and Pt/Ag/Fe the diffusion path is initially mainly driven by the preferred Pt–Ag intermixing and facilitated by the mutual insolubility of Ag and Fe.

Table 1
Values of enthalpy of mixing $\Delta H^{mix}_{(AB)}$ for atomic pairs calculated by Miedema's model.

Atomic pair	$\Delta H^{mix}_{(AB)}$, kJ/mol
Au–Pt	4
Pt–Ag	−1
Fe–Pt	−13
Au–Fe	8
Ag–Fe	28

4. Conclusions

In this work, we studied the diffusion-driven phase formation of the chemically ordered $L1_0$ FePt phase upon post-annealing at 700 °C in Fe (15 nm)/Ag(Au)/Pt(15 nm) and Pt(15 nm)/Ag(Au)/Fe(15 nm) trilayers employing a 10 nm thick Ag(Au) interlayer. It is shown that in trilayers using Au the $L1_0$ FePt phase formation is enhanced compared to trilayers using Ag. Depending on the layer stacking, rather different diffusion paths are obtained. Finally, after annealing for 30 min, the formation of an almost homogenous hard magnetic $L1_0$ FePt phase containing Ag(Au) in the grain boundaries is observed. In addition, Au(Ag) also segregates at the top surface or the substrate interface depending on the layer stacking and their mutual solubility. Interestingly, a similar evolution of the depth profiles upon annealing resulting in a comparable microstructure are observed for Fe/Ag/Pt and Pt/Au/Fe as well as for Pt/Ag/Fe and Fe/Au/Pt trilayers, which is due to strong Pt–Ag and Fe–Au initial intermixing. Corresponding to the similar microstructure and degree of chemical ordering similar coercivities of 1048 kA/m (Fe/Ag/Pt)/1024 kA/m (Pt/Au/Fe) and 848 kA/m (Pt/Ag/Fe)/856 kA/m (Fe/Au/Pt) were observed for the post-annealed trilayers. In this regard, employing different diffusion paths on selected layer stacks is a promising approach of forming for instance magnetic gradient nanomaterials with varying magnetic properties along the film thickness which might be useful for applications.

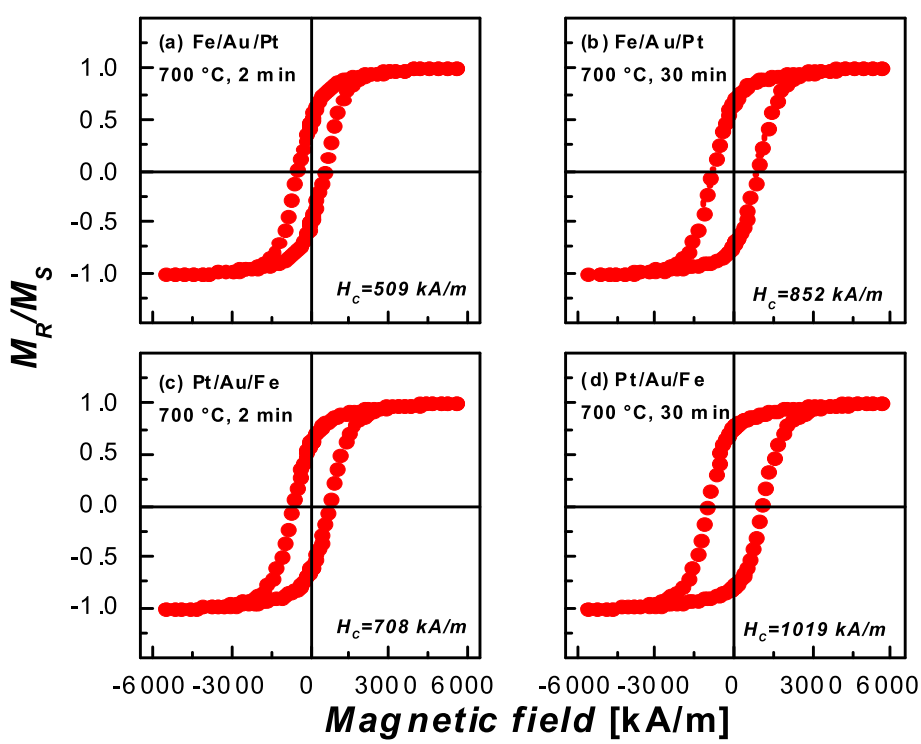

Fig. 6. Out-of-plane hysteresis loops of (a, b) Fe(15 nm)/Au(10 nm)/Pt(15 nm) and (c, d) Pt(15 nm)/Au(10 nm)/Fe(15 nm) films after post-annealing at 700 °C for 2 min and 30 min, respectively.

CRediT authorship contribution statement

G.L. Katona: Methodology, Conceptualization. **P.V. Makushko:** Investigation. **N.Y. Schmidt:** Writing – review & editing, Writing – original draft, Methodology, Investigation, Conceptualization. **O. Lik:** Methodology, Investigation. **T.I. Verbytska:** Writing – review & editing, Writing – original draft, Methodology, Investigation, Formal analysis. **G. Beddies:** Methodology, Investigation. **D.L. Beke:** Methodology, Investigation. **M. Albrecht:** Writing – review & editing, Writing – original draft, Methodology, Investigation, Conceptualization. **Yu.M. Makogon:** Writing – review & editing, Writing – original draft, Methodology, Investigation, Formal analysis, Conceptualization.

Declaration of competing interest

The authors declare that they have no known competing financial interests or personal relationships that could have appeared to influence the work reported in this paper.

Acknowledgement

This work was financially supported by the German Academic Exchange Service (DAAD) in the frame of the Leonard-Euler scholarship program (grant IDs 57551511, 57590076, 57630758).

Data availability

Data will be made available on request.

References

[1] Weller, Dieter, Mosendz, Oleksandr, Parker, Gregory, Pisana, Simone, Santos, Tiffany S., 2013. $L1_0$ FePtX–Y media for heat-assisted magnetic recording: a review. Phys. Status Solidi A 210, 1245–1260. https://doi.org/10.1002/pssa.201329106.

[2] Weller, Dieter, Parker, Gregory, Mosendz, Oleksandr, Lyberatos, Andreas, Mitin, Dmitriy, Safonova, Nataliia Y., Albrecht, Manfred, 2016. Review article: FePt heat assisted magnetic recording media. J. Vac. Sci. Technol. B 34, 60801. https://doi.org/10.1116/1.4965980.

[3] Piramanayagam, S.N., Chong, T.C. (Eds.), 2011. Development in Data Storage: Materials Perspective. Wiley, New York, p. 352. ISBN 978-0-470-50100-9. https://www.researchgate.net/publication/274081153.

[4] Varaprasad, B.S.D.ChS., Takahashi, Y.K., Wang, J., Ina, T., Nakamura, T., Ueno, W., Nitta, K., Uruga, T., Hono, K., 2014. Mechanism of coercivity enhancement by Ag addition in FePt-C granular films for heat assisted magnetic recording media. Appl. Phys. Lett. 104, 222403. https://doi.org/10.1063/1.4880655.

[5] Brombacher, C., Grobis, M., Lee, J., Fidler, J., Eriksson, T., Werner, T., Hellwig, O., Albrecht, M., 2012. $L1_0$ FePtCu bit patterned media. Nanotechnology 23, 025301. https://doi.org/10.1088/0957-4484/23/2/025301.

[6] Mitin, D., Wachs, M., Safonova, N.Y., Klein, O., Albrecht, M., 2018. Exchange coupled $L1_0$ FeCuPt/Fe heterostructures: magnetic properties and reversal behavior at elevated temperatures. Thin Solid Films 651, 158–162. https://doi.org/10.1016/j.tsf.2017.06.059.

[7] Brombacher, C., Schletter, H., Daniel, M., Matthes, P., Jöhrmann, N., Maret, M., Makarov, D., Hietschold, M., Albrecht, M., 2012. FePtCu alloy thin films: morphology, $L1_0$ chemical ordering, and perpendicular magnetic anisotropy. J. Appl. Phys. 112, 073912. https://doi.org/10.1063/1.4757038.

[8] Maret, M., Brombacher, C., Matthes, P., Makarov, D., Boudet, N., Albrecht, M., 2012. Anomalous x-ray diffraction measurements of long-range order in (001)-textured $L1_0$ FePtCu thin films. Phys. Rev. B 86, 024204. https://doi.org/10.1103/PhysRevB.86.024204.

[9] Singh, S., Prajapat, C.L., Gupta, M., Basu, S., 2018. Room temperature superparamagnetism in ternary $(Fe_{50}Pt_{50})_{0.42}Cu_{0.58}$ phase at interfaces on annealing of $Fe_{50}Pt_{50}$/Cu multilayer. J. Magn. Magn. Mater. 462, 58–69. https://doi.org/10.1016/j.jmmm.2018.05.008.

[10] Basha, M.A., Bhatt, H., Kumar, Y., Prajapat, C.L., Gupta, M., Karki, V., Basu, S., Singh, S., 2020. Annealing driven positive and negative exchange bias in Fe–Cu–Pt heterostructures at room temperature. J. Alloys Compd. 815, 152640. https://doi.org/10.1016/j.jallcom.2019.152640.

[11] Basha, M.A., Bhatt, H., Kumar, Y., Prajapat, C.L., Gupta, M., Karki, V., Ghosh, S.K., Basu, S., Singh, S., 2020. Evolution of structural and magnetic properties of FePtCu alloy films on annealing of FePt/Cu multilayers. Phys. Chem. Chem. Phys. 22, 16107–16116. https://doi.org/10.1039/D0CP02484H.

[12] Kumar, S., Srihari, V., Sharma, G., Gupta, A., Reddy, V.R., Gupta, M., Gome, A., Sharma, K., 2023. Cu interfaced Fe/Pt multilayer with improved (001) texture, enhanced $L1_0$ transformation kinetics and high magnetic anisotropy. J. Magn. Magn. Mater. 567, 170327. https://doi.org/10.1016/j.jmmm.2022.170327.

[13] Platt, C.L., Wierman, K.W., Svedberg, E.B., Veerdonk, R.van de, Howard, J.K., Roy, A.G., Laughlin, D.E., 2002. $L1_0$ ordering and microstructure of FePt thin films with Cu, Ag, and Au additive. J. Appl. Phys. 92, 6104–6109. https://doi.org/10.1063/1.1516870.

[14] Lee, S.R., Yang, S., Kim, Y.K., Na, J.G., 2001. Rapid ordering of Zr-doped FePt alloy films. Appl. Phys. Lett. 78, 4001–4003. https://doi.org/10.1063/1.1379591.

[15] Zhang, W.Y., Shima, H., Takano, F., Akinaga, H., Yu, X.Z., Hara, T., Zhang, W.Z., Kimoto, K., Matsui, Y., Nimori, S., 2009. Enhancement in ordering of $Fe_{50}Pt_{50}$ film caused by Cr and Cu additives. J. Appl. Phys. 106, 033907. https://doi.org/10.1063/1.3194313.

[16] Takahashi, Y.K., Ohnuma, M., Hono, K., 2002. Effect of Cu on the structure and magnetic properties of FePt sputtered film. J. Magn. Magn. Mater. 246, 259–265. https://doi.org/10.1016/S0304-8853(02)00065-3.

[17] Kitakami, O., Shimada, Y., Oikawa, K., Daimon, H., Fukamichi, K., 2001. Low-temperature ordering of $L1_0$–CoPt thin films promoted by Sn, Pb, Sb, and Bi additives. Appl. Phys. Lett. 78, 1104–1106. https://doi.org/10.1063/1.1346628.

[18] Chen, C., Kitakami, O., Okamoto, S., Shimada, Y., 2000. Ordering and orientation of CoPt/SiO_2 granular films with additive Ag. Appl. Phys. Lett. 76, 3218–3220. https://doi.org/10.1063/1.126634.

[19] Tokuoka, Y., Seto, Y., Kato, T., Iwata, S., 2014. Effect of Ag addition to $L1_0$ FePt and $L1_0$ FePd films grown by molecular beam epitaxy. J. Appl. Phys. 115, 17B716. https://doi.org/10.1063/1.4864251.

[20] You, C.Y., Takahashi, Y.K., Hono, K., 2006. Particulate structure of FePt thin films enhanced by Au and Ag alloying. J. Appl. Phys. 100, 056105. https://doi.org/10.1063/1.2335600.

[21] Feng, C., Zhan, Q., Li, B., Teng, J., Li, M., Jiang, Y., Yu, G., 2008. Magnetic properties and microstructure of FePt/Au multilayers with high perpendicular magnetocrystalline anisotropy. Appl. Phys. Lett. 93, 152513. https://doi.org/10.1063/1.3001801.

[22] Zhu, Y., Cai, J.W., 2005. Low-temperature ordering of FePt thin films by a thin AuCu underlayer. Appl. Phys. Lett. 87, 032504. https://doi.org/10.1063/1.1997268.

[23] Seki, T.O., Takahashi, Y.K., Hono, K., 2008. Microstructure and magnetic properties of FePt-SiO_2 granular films with Ag addition. J. Appl. Phys. 103, 023910. https://doi.org/10.1063/1.2828032.

[24] Vladymyrskyi, I.A., Pavlova, O.P., Verbitska, T.I., Sidorenko, S.I., Katona, G.L., Beke, D.L., Makogon, Iu.M., 2014. Influence of intermediate Ag layer on the structure and magnetic properties of Pt/Ag/Fe thin films. Vacuum 101, 33–37. https://doi.org/10.1016/j.vacuum.2013.07.018.

[25] Pavlova, O.P., Verbitska, T.I., Vladymyrskyi, I.A., Sidorenko, S.I., Katona, G.L., Beke, D.L., Beddies, G., Albrecht, M., Makogon, Iu.M., 2013. Structural and magnetic properties of annealed FePt/Ag/FePt thin films. Appl. Surf. Sci. 266, 100–104. https://doi.org/10.1016/j.apsusc.2012.11.102.

[26] Makushko, P.V., Verbytska, M.Yu, Shamis, M.N., Verbytska, T.I., Beddies, G., Safonova, N.Y., Albrecht, M., Makogon, IuN., 2020. Effect of initial stress/strain state on the $L1_0$ phase formation of FePt in FePt/Au/FePt trilayers. Appl. Nanosci. 10, 2775–2780. https://doi.org/10.1007/s13204-019-01066-6.

[27] Katona, G.L., Vladymyrskyi, I.A., Makogon, I.M., Sidorenko, S.I., Kristály, F., Daróczi, L., Csik, A., Liebig, A., Beddies, G., Albrecht, M., Beke, D.L., 2014. Grain boundary diffusion induced reaction layer formation in Fe/Pt thin films. Appl. Phys. A Mater. Sci. Process. 115, 203–211. https://doi.org/10.1007/s00339-013-7949-z.

[28] Katona, G.L., Safonova, N.Y., Ganss, F., Mitin, D., Vladymyrskyi, I.A., Sidorenko, S. I., Makogon, Iu.M., Beddies, G., Albrecht, M., Beke, D.L., 2015. Diffusion and solid state reactions in Fe/Ag/Pt and FePt/Ag thin-film systems. J. Phys. D Appl. Phys. 48, 175001. https://doi.org/10.1088/0022-3727/48/17/175001.

[29] Goyal, R., Lamba, S., Annapoorni, S., 2019. Modelling of strain induced magnetic anisotropy in Au additive FePt thin films. Prog. Nat. Sci. Mater. Int. 29, 517–524. https://doi.org/10.1016/j.pnsc.2019.09.001.

[30] Wang, B., Barmak, K., Klemmer, T.J., 2010. A1 to $L1_0$ transformation in FePt films with ternary alloying of Ag and Au. IEEE Trans. Magn. 46 (6), 1773–1776. https://doi.org/10.1109/TMAG.2010.2042039.

[31] Vladymyrskyi, I.A., Gafarov, A.E., Burmak, A.P., Sidorenko, S.I., Katona, G.L., Safonova, N.Y., Ganss, F., Beddies, G., Albrecht, M., Makogon, Iu.M., Beke, D.L., 2016. Low-temperature formation of the FePt phase in the presence of an intermediate Au layer in Pt/Au/Fe thin films. J. Phys. D Appl. Phys. 49, 035003. https://doi.org/10.1088/0022-3727/49/3/035003.

[32] Vladymyrskyi, I.A., Mamchur, Y., Dubikovskyi, O.V., Voloshko, S.M., Ullrich, A., Albrecht, M., 2022. Phase composition and magnetic properties of post-annealed asymmetric Pt/Fe/Pt/Au/Fe thin films. Thin Solid Films 754, 139300. https://doi.org/10.1016/j.tsf.2022.139300.

[33] Gulyás, S., Katona, G.L., 2024. Structural and phase transformations in Fe-Pd-Ag layered thin films by grain boundary diffusion. Phys. Scri. 99, 095970. https://doi.org/10.1088/1402-4896/ad6d9f.

[34] Gulyás, S., Katona, G.L., 2024. Effect of Mo and W underlayers on ordered phase formation in Fe-Au-Pd multilayer thin films at low temperatures. Heliyon 10 (12), e32865. https://doi.org/10.1016/j.heliyon.2024.e32865.

[35] Pedan, R., Makushko, P., Yavorskyi, Yu, Dubikovskyi, O., Bodnaruk, A., Burmak, A., Golub, V., Voloshko, S., Hübner, R., Makarov, D., Vladymyrskyi, I., 2024. Low-temperature diffusion in thin-film Pt-(Au)-Co heterostructures: a structural and magnetic characterization. Nanotechnology 35, 195707. https://doi.org/10.1088/1361-6528/ad22a8.

[36] Oechsner, H., Getto, R., Kopnarski, M., 2009. Quantitative characterization of solid state phases by secondary neutral mass spectrometry. J. Appl. Phys. 105, 063523. https://doi.org/10.1063/1.3099595.

[37] Im, E., Kim, S., 2024. Magnetic and crystallographic properties of $L1_0$ FePt thin films in contact with Ta and Pt layers. J. Sens. Sci. Technol. 33 (6), 487–492. https://doi.org/10.46670/JSST.2024.33.6.487.

[38] Takeuchi, A., Inoue, A., 2005. Classification of bulk metallic glasses by atomic size difference, heat of mixing and period of constituent elements and its application to characterization of the main alloying element. Mater. Trans. 46 (12), 2817–2829. https://doi.org/10.2320/matertrans.46.2817.